

Combinatorial Study of Ceramic Tape-Casting Slurries

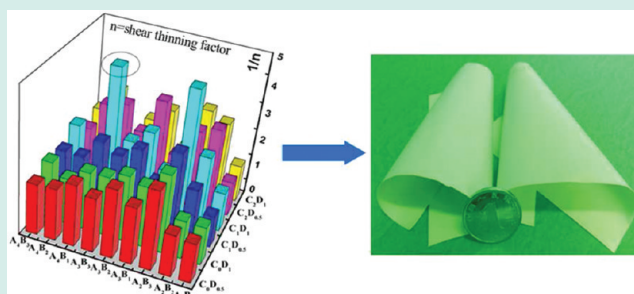
Zhifu Liu,* Yiling Wang, and Yongxiang Li*

The Key Laboratory of Inorganic Functional Materials and Devices, Shanghai Institute of Ceramics, Chinese Academy of Sciences, 1295 Dingxi Road, Shanghai 200050, China

S Supporting Information

ABSTRACT: Ceramic tape-casting slurries are complex systems composed of ceramic powder, solvent, and a number of organic components. Conventionally, the development of ceramic tape-casting slurries is time-consuming and of low efficiency. In this work, combinatorial approaches were applied to screen the ethanol and ethyl-acetate binary solvent based slurry for ceramic green tape-casting. The combinatorial libraries were designed considering the variation of the amount of PVB (Poly vinyl-butylal) binder, polyethylene-400, and butyl-benzyl-phthalate plasticizers, and glyceryl triacetate dispersant. A parallel magnetic stirring process was used to make the combinatorial slurry library. The properties mapping of the slurry library was obtained by investigating the sedimentation and rheological characteristics of the slurries. The slurry composition was refined by scaling up the experiments and comparing the microstructure, mechanical property, and sintering behavior of green tapes made from the selected slurries. Finally, a kind of ethanol-ethyl acetate binary solvent based slurry system suitable for making X7R dielectric ceramic green tapes was achieved.

KEYWORDS: tape-casting, slurry, combinatorial library, rheological property



1. INTRODUCTION

Tape-casting, a technique established more than 60 years ago, is widely used as manufacturing process for multilayer ceramics packaging substrates, solid oxide fuel cell (SOFC) anodes, battery separator, functional graded materials, and numerous components and devices such as multilayer ceramics capacitors (MLCC), piezoelectric actuators, and gas sensors.^{1–3} During ceramic green tape-casting, the slurry consisting of the ceramic powder in solvent, with addition of dispersants, binders, and plasticizers, is cast onto a stationary or moving surface. The ceramic green tape can be obtained after a drying procedure. Since ceramic green tape needs to endure punching, electrode paste screen-printing, lamination, debinding, and sintering steps to obtain multilayer structures, the green tapes must possess dimensional stability and mechanical integrity, which largely depend on the tape-casting slurry. Therefore, the development of a high quality ceramic tape-casting slurry is one of the main topics in ceramics processing.

The ceramic tape-casting slurry is a complex mixture system of ceramic powder, solvent, binder, dispersant, plasticizer, defoamer, and other agents. The composition of the tape-casting slurry concerning type and amount of solvent, binder, dispersant, and plasticizer were chosen as the most important factors affecting the quality and the processing properties of the ceramic green tape. Generally, the amount and even the type of organic components in a slurry system should be adjusted to fit each given ceramic powder to obtain high quality green tape. In addition, in recent years, the more strict environmental regulation requires the use of environmentally friendly solvents

to replace the toxic ones such as MEK, toluene, and xylene. Therefore, the development of an environmentally friendly new slurry system is in demand. However, because of the large number of parameters, quite a number of experiments should be carried out to optimize the type and amount of the slurry components for obtaining the ceramic tape-casting slurry. Therefore, it is desirable to reduce the number of experiments or to improve the efficiency in the development of tape-casting slurry. Design of experiment (DOE) is an effective tool to discover the complex interrelations among several influencing factors.⁴ In recent years, the DOE approach has been used in the development of ceramic green tapes.^{5–9} Research works based on the DOE method extended from tape-casting composition optimization to the investigation of the factors influencing ceramic tape sintering properties. However, the DOE approach optimizes experimental parameters using statistical analysis and is an indirect method.

Combinatorial technology has been increasingly applied for the discovery and optimization of superconductor oxides,¹⁰ phosphors,^{11–13} catalysts,¹⁴ alloys,¹⁵ dielectric materials,^{16,17} piezoelectric ceramics,^{18,19} and so forth for more than one decade. Benefitting from various parallel experimental strategies and modern experimental techniques, the combinatorial approach makes it possible to develop new materials or optimize processing parameters in a faster, cheaper, and more

Received: September 7, 2011

Revised: October 29, 2011

Published: January 27, 2012

effective way. However, there is no report on the application of the combinatorial method to the complex ceramic slurry study. In this work, we introduce the combinatorial technology to the development of ceramic tape-casting slurry. The slurry composition is optimized by monitoring the rheology, stability of the slurry, and the drying characteristics, morphology, density, strength, and the sintering characteristics of green tapes.

2. EXPERIMENTAL PROCEDURES

The ceramic slurries are composed of X7R ceramic powder (GC-292M, Sinocera Co., Dongyin, China) (Cera) with a mean particle size of 0.6 μm and organic components. The mixture of ethanol and ethyl-acetate (1:1 mass ratio) was used as solvent (Sol). Poly vinyl-butylal (PVB) (B06SY, CCP, TaiWan) was used as binder (A). Polyethylene-400 (PEG400) (B) and butyl-benzyl-phthalate (BBP) (C) were used as plasticizers. Glyceryl triacetate was used as dispersant (D). So the composition of the slurry can be written as $\text{Cera}_m\text{Sol}_n\text{A}_w\text{B}_x\text{C}_y\text{D}_z$, where m , n , w , x , y , and z indicate the amount of each component. To prepare the slurry, the ceramic powder is first mixed with the solvent and dispersant. After a homogeneous mixture is obtained, the PVB binder and the plasticizers are added, and then, the mixture is mixed further to form a homogeneous stable slurry.

In the first step screening, 60 g ceramic powder ($m = 60$) and 20 g solvent ($n = 20$) were used for each sample. For the amounts of PVB binder, PEG400, BBP, and the dispersant, $w = 2, 3, 4$; $x = 1, 2, 3$; $y = 0, 1, 2$; $z = 0.5, 1$ (the unit is gram for all) were selected, respectively. The composition of the sample can be written as $\text{Cera}_{60}\text{Sol}_{20}\text{A}_w\text{B}_x\text{C}_y\text{D}_z$ if, for example, $w = 2$ g; $x = 1$ g; $y = 0$ g; $z = 0.5$ g are selected. So the combinatorial library contains 54 samples for the first stage of screening. The samples were prepared parallel by magnetic stirring in covered plastic bottles for 4 h first and then 10 h after the binder and plasticizers were added (see the Supporting Information for details). In the second step screening, 4-fold ceramic powder was used. The amount of each organic component was increased correspondingly. The mixture of ceramic powder, solvent, and dispersant was milled with ZrO_2 balls in a Teflon pot for 4 h and then 10 h after the binder and plasticizers were added. Lastly, the slurries were filtered and degassed for tape-casting and properties testing.

The viscosity and shear strength were measured using a NDJ-79 (CNSHP, China) rheometer. The stability of the slurries was checked by a sedimentation experiment (see the Supporting Information for details). The rheological characteristics of the slurries were investigated by a Physica MCR301 rheometer (Anton Paar, Austria). The ceramic green tapes were prepared on a CAM-20 casting machine (KEKO Equipment Ltd., Slovenia). A JSM-6700F field emission scanning electron microscope (FESEM) (JEOL, Japan) was used to observe the morphology of the green tapes. The tensile strength of the tapes was tested on an INSTRON 5566 mechanical testing system (INSTRON, U.S.A.). The density of the green tapes was measured according to Archimedes' law. To investigate the sintering shrinkage, the green tapes were debinded at 450 $^\circ\text{C}$ for 2 h and sintered at 1050 $^\circ\text{C}$ for 4 h.

3. RESULTS AND DISCUSSION

To make uniform dense green tapes, the tape-casting slurry should be a well dispersed stable system with good shear

shining behavior and high solid loading. Normally, the preparation of ceramic tape-casting slurry needs milling for a long time to obtain good homogeneity and stability. So the slurry preparation is one of the bottlenecks of efficient slurry composition screening. Magnetic stirring is a conventional, easy method for preparing the mixture solution. Preliminary experiments indicated that the properties of the slurry prepared by magnetic stirring have good repeatability and comparability. In this work, we prepared the combinatorial libraries by parallel mixing samples using multiposition magnetic stirrers, which allow high throughput preparation of the slurry samples for the next step examination.

The stability and the rheological characteristics are important parameters of tape-casting slurry. A sedimentation test is normally used to check the stability of the slurry, and a low settling rate represents a high degree of dispersion and therefore a good stability. To investigate the effect of the slurry composition on the slurry stability, the slurry library was settled for one month. Figure 1 shows the volume ratio of the

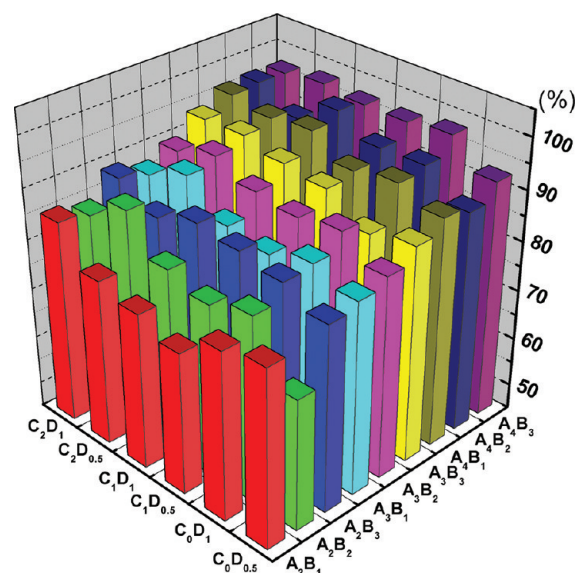


Figure 1. Volume ratio of the homogeneous part of the $\text{Cera}_{60}\text{Sol}_{20}\text{A}_w\text{B}_x\text{C}_y\text{D}_z$ slurry library after settling for one month, where $w = 2, 3, 4$; $x = 1, 2, 3$; $y = 0, 1$; $z = 0.5, 1$.

homogeneous slurry part of the $\text{Cera}_{60}\text{Sol}_{20}\text{A}_w\text{B}_x\text{C}_y\text{D}_z$ ($w = 2, 3, 4$; $x = 1, 2, 3$; $y = 0, 1$; $z = 0.5, 1$) slurry library after settling for one month. There is an obvious trend that the slurry stability gets better with the increase of the amount of "A" component, the PVB binder. The increase of component "C", PEG400, also improves the stability of the slurry. Although the PVB acts as binder and the PEG400 acts as plasticizer in the slurry system, the covering of stretched polymers like PVB and PEG400 on the well dispersed ceramic particles would increase the interaction between the particles.^{20,21} Therefore, it is understandable that the slurry stability could be improved with the increase of PVB and PEG400 amounts. The effect on the stability is not very obvious when the amount of dispersant "D" was changed from 0.5 to 1 g. But experiment indicates that the stability of the slurry is much worse if the amount of "D" is zero. So the dispersant should have a large effect on the deagglomeration of ceramic particles during the first stage mixing. However, this effect may be overwhelmed by the addition of binder and plasticizers.

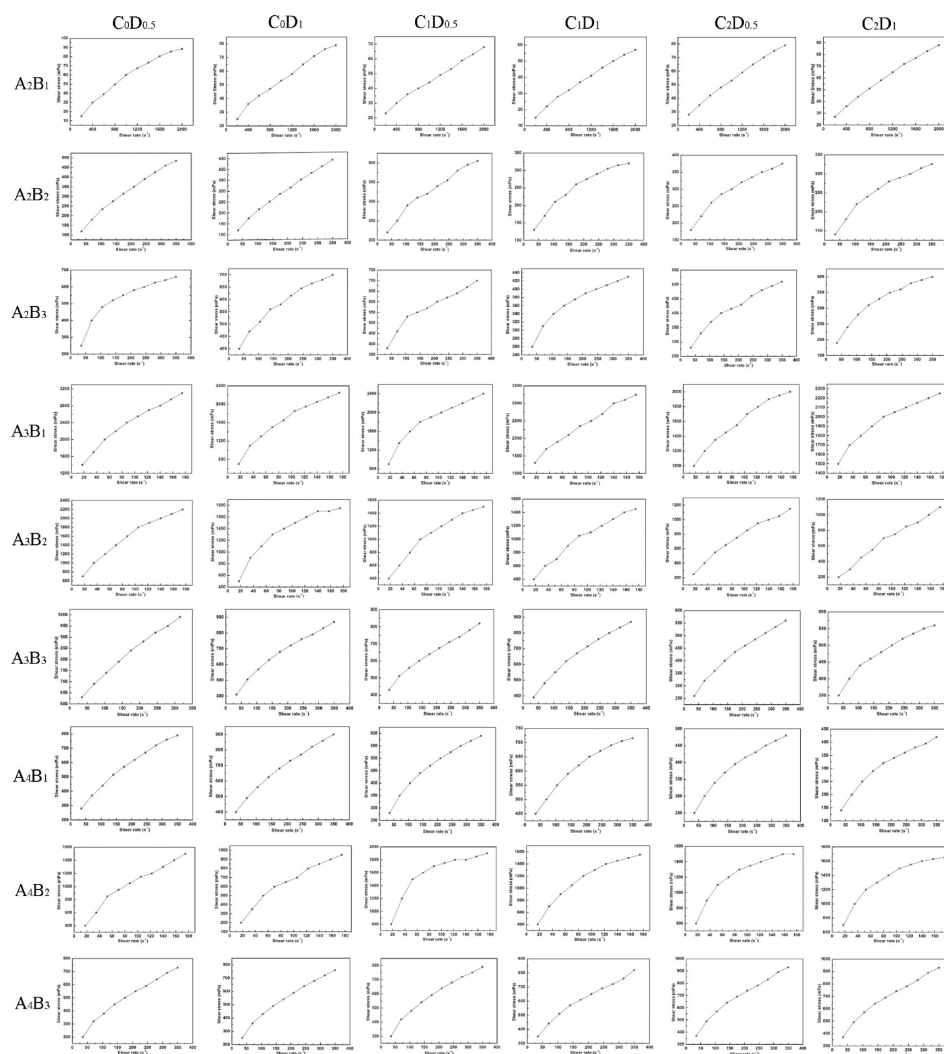


Figure 2. Shear stress versus shear rate curves of the $\text{Cera}_{60}\text{Sol}_{20}\text{A}_w\text{B}_x\text{C}_y\text{D}_z$ slurry library, where $w = 2, 3, 4$; $x = 1, 2, 3$; $y = 0, 1$; $z = 0.5, 1$.

The rheological characteristic is a visual representation of the interaction of organic components with the ceramics particles in the slurry. So the rheological property is one of the most important criterions for screening the slurry composition. Figure 2 presents the shear stress versus shear rate curves of the $\text{Cera}_{60}\text{Sol}_{20}\text{A}_w\text{B}_x\text{C}_y\text{D}_z$ slurry library samples. It can be seen that the functions between shear stress and shear rate of all samples follow power law with an index less than one. That means these slurries show non-Newtonian behavior and are shear thinning fluids. This kind of behavior indicates the presence of pseudostructure as a result of the entanglement of stretched PVB chains. The pseudostructure is readily broken down under the shear force applied, and the fluidity of the slurry is improved.²²

Good shear thinning property allows the slurry to have excellent fluidity when experiencing shear force under the action of carrier/blade moving during the casting process. The viscosity of the slurry recovers just after the slurry is past the blade so that a uniform green tape can be obtained. To have a better understanding of the rheological properties of the slurries, the shear stress versus shear rate curves were analyzed further. According to the Herschel–Bulkley model,²³ the

relationship between shear stress (τ) and shear rate ($\dot{\gamma}$) can be written as

$$\tau = \tau_y + K\dot{\gamma}^n \quad (1)$$

where τ_y is the yield shear stress needed to initiate flow; K is the consistency index; n is the shear thinning constant. Values of $n < 1$ correspond to a shear thinning or pseudoplastic behavior. To compare the shear thinning property of the $\text{Cera}_{60}\text{Sol}_{20}\text{A}_w\text{B}_x\text{C}_y\text{D}_z$ slurry library quantitatively, the shear stress versus shear rate curves were fitted with the Herschel–Bulkley model so that the shear thinning constant “ n ” of each slurry could be obtained. Figure 3 compared the shear thinning constants of the slurries in the $\text{Cera}_{60}\text{Sol}_{20}\text{A}_w\text{B}_x\text{C}_y\text{D}_z$ slurry library. To have a good visibility, the $1/n$ values were presented in the figure. It can be seen that the $1/n$ values changes largely with the variation of the composition of the slurry system. But the shear thinning constant does not show obvious dependence on any single component of the slurry. This implies the complexity of the interaction in the slurry system, and the rheological behavior of the slurry is a general result of the interaction of solvent, dispersant, binder, and plasticizers. The shear thinning constant of $\text{Cera}_{60}\text{Sol}_{20}\text{A}_2\text{B}_3\text{C}_2\text{D}_1$, $\text{Cera}_{60}\text{Sol}_{20}\text{A}_3\text{B}_2\text{C}_2\text{D}_{0.5}$, $\text{Cera}_{60}\text{Sol}_{20}\text{A}_4\text{B}_1\text{C}_1\text{D}_1$, and $\text{Cera}_{60}\text{Sol}_{20}\text{A}_4\text{B}_1\text{C}_2\text{D}_1$ slurry system is 0.209, 0.281, 0.206, and

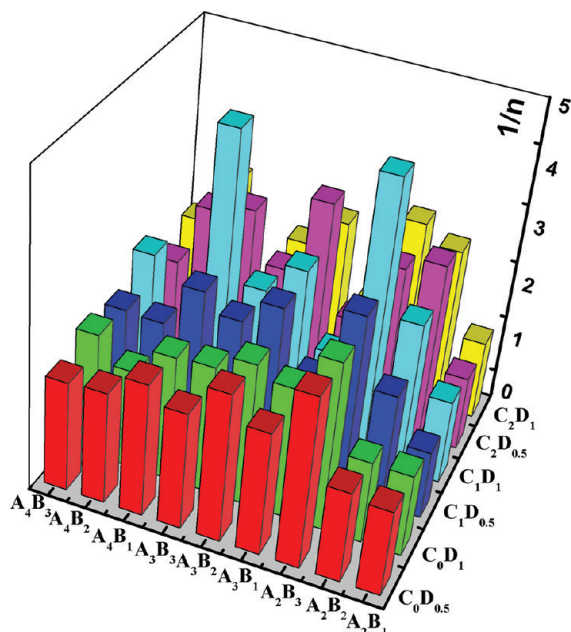


Figure 3. Comparison of the shear thinning constants of the $\text{Cera}_{60}\text{Sol}_{20}\text{A}_w\text{B}_x\text{C}_y\text{D}_z$ slurry library, where $w = 2, 3, 4$; $x = 1, 2, 3$; $y = 0, 1$; $z = 0.5, 1$. The $1/n$ is used here for a good visibility.

0.316, respectively, which are the lowest values in the slurry library. That is to say, these four slurry systems show the strongest shear thinning behavior in the slurry library.

On the basis of the stability and the rheological characteristics study, the $\text{Cera}_{60}\text{Sol}_{20}\text{A}_2\text{B}_3\text{C}_2\text{D}_1$, $\text{Cera}_{60}\text{Sol}_{20}\text{A}_3\text{B}_2\text{C}_2\text{D}_{0.5}$, $\text{Cera}_{60}\text{Sol}_{20}\text{A}_4\text{B}_1\text{C}_1\text{D}_1$, and $\text{Cera}_{60}\text{Sol}_{20}\text{A}_4\text{B}_1\text{C}_2\text{D}_1$ slurry systems are suitable for tape-casting and were selected to be investigated in more detail. In the second step screening, 4-fold of the ceramic powder and organic components were used. The slurries were prepared by ball milling and were filtered and degassed before tape-casting and properties testing.

Figure 4 shows the viscosity depending on the shear rate of the $\text{Cera}_{60}\text{Sol}_{20}\text{A}_2\text{B}_3\text{C}_2\text{D}_1$, $\text{Cera}_{60}\text{Sol}_{20}\text{A}_3\text{B}_2\text{C}_2\text{D}_{0.5}$, Ce-

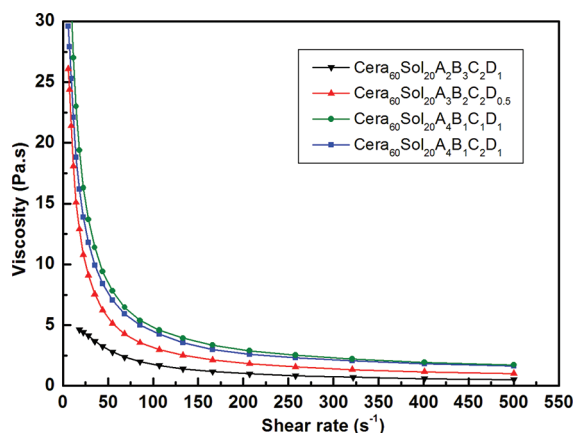


Figure 4. Viscosity depending on the shear rate of the $\text{Cera}_{60}\text{Sol}_{20}\text{A}_2\text{B}_3\text{C}_2\text{D}_1$, $\text{Cera}_{60}\text{Sol}_{20}\text{A}_3\text{B}_2\text{C}_2\text{D}_{0.5}$, $\text{Cera}_{60}\text{Sol}_{20}\text{A}_4\text{B}_1\text{C}_1\text{D}_1$, and $\text{Cera}_{60}\text{Sol}_{20}\text{A}_4\text{B}_1\text{C}_2\text{D}_1$ slurry systems.

$\text{ra}_{60}\text{Sol}_{20}\text{A}_4\text{B}_1\text{C}_1\text{D}_1$, and $\text{Cera}_{60}\text{Sol}_{20}\text{A}_4\text{B}_1\text{C}_2\text{D}_1$ slurry systems. The viscosity curves show typical non-Newtonian behavior and exhibit strong shear thinning behavior in the 10–500 s^{-1} shear rate region. The slurries $\text{Cera}_{60}\text{Sol}_{20}\text{A}_4\text{B}_1\text{C}_1\text{D}_1$ and Ce-

$\text{ra}_{60}\text{Sol}_{20}\text{A}_4\text{B}_1\text{C}_2\text{D}_1$ have similar viscosity, which is larger than that of the slurries $\text{Cera}_{60}\text{Sol}_{20}\text{A}_2\text{B}_3\text{C}_2\text{D}_1$ and $\text{Cera}_{60}\text{Sol}_{20}\text{A}_3\text{B}_2\text{C}_2\text{D}_{0.5}$. We noticed that the plasticizers/binder ratios of $\text{Cera}_{60}\text{Sol}_{20}\text{A}_2\text{B}_3\text{C}_2\text{D}_1$, $\text{Cera}_{60}\text{Sol}_{20}\text{A}_3\text{B}_2\text{C}_2\text{D}_{0.5}$, $\text{Cera}_{60}\text{Sol}_{20}\text{A}_4\text{B}_1\text{C}_1\text{D}_1$, and $\text{Cera}_{60}\text{Sol}_{20}\text{A}_4\text{B}_1\text{C}_2\text{D}_1$ slurry system are 2.5, 1.3, 0.5, and 0.75, respectively. As is known, the plasticizers in the slurry can reduce the frictional force between PVB chains or break down the network structure formed by PVB chains because of a decrease of the attractive interaction between PVB chains.²⁴ So it is understandable that the higher plasticizer/binder ratio leads to a lower viscosity of the slurry.

Green ceramic tapes with thickness of about 100 μm were obtained by casting the slurries on the CAM-200 automatic tape-casting machine. Uniform and flexible green tapes were obtained from all the four slurries. Figure 5 is the photograph of

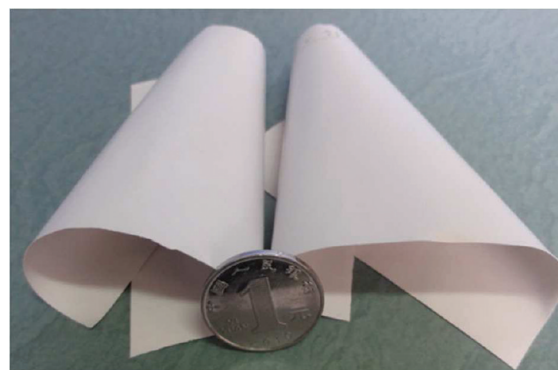


Figure 5. Flexible green tape obtained from $\text{Cera}_{60}\text{Sol}_{20}\text{A}_4\text{B}_1\text{C}_1\text{D}_1$ slurry.

the flexible green tape obtained from the $\text{Cera}_{60}\text{Sol}_{20}\text{A}_4\text{B}_1\text{C}_1\text{D}_1$ slurry. As shown in Table 1, the ceramic powder loading in the green tapes is 67.01, 65.32, 64.00, and 63.41 wt % for the tapes made from $\text{Cera}_{60}\text{Sol}_{20}\text{A}_2\text{B}_3\text{C}_2\text{D}_1$, $\text{Cera}_{60}\text{Sol}_{20}\text{A}_3\text{B}_2\text{C}_2\text{D}_{0.5}$, $\text{Cera}_{60}\text{Sol}_{20}\text{A}_4\text{B}_1\text{C}_1\text{D}_1$, and $\text{Cera}_{60}\text{Sol}_{20}\text{A}_4\text{B}_1\text{C}_2\text{D}_1$ slurry systems, respectively. The corresponding green tape density is 3.67, 3.65, 3.35, and 3.37 g/cm^3 .

The microstructure of the green tapes was observed by SEM and is represented in Figure 6. The tape made from $\text{Cera}_{60}\text{Sol}_{20}\text{A}_2\text{B}_3\text{C}_2\text{D}_1$ shows a little rough and porous structure on the surface. While, the tapes made from other three slurry systems have smooth and well-packed surface morphology. Previous results show that the $\text{Cera}_{60}\text{Sol}_{20}\text{A}_2\text{B}_3\text{C}_2\text{D}_1$ slurry has the lowest viscosity among the slurries investigated and has good homogeneity. So the porous surface morphology cannot be explained from the slurry dispersion nonuniformity. Another possible factor is the tape-casting process. It is known that the shrinkage control at the drying stage is very important for achieving a dense green tape.¹ We noticed that the $\text{Cera}_{60}\text{Sol}_{20}\text{A}_2\text{B}_3\text{C}_2\text{D}_1$ slurry contains ceramic powder up to 67.01 wt %. But the ratio of binder is only about 2 wt %. The binder is not enough for covering all the ceramic particles and holding ceramic particles together when the shrinkage occurs. So small crack or pores may form in the green tape during the drying process of the tape-casting. This kind of porous structure leads to low strength as confirmed by the mechanical property characterization.

The tensile strength-strain curves of the green tapes obtained from the slurries $\text{Cera}_{60}\text{Sol}_{20}\text{A}_2\text{B}_3\text{C}_2\text{D}_1$, $\text{Cera}_{60}\text{Sol}_{20}\text{A}_3\text{B}_2\text{C}_2\text{D}_{0.5}$, $\text{Cera}_{60}\text{Sol}_{20}\text{A}_4\text{B}_1\text{C}_1\text{D}_1$, and $\text{Cera}_{60}\text{Sol}_{20}\text{A}_4\text{B}_1\text{C}_2\text{D}_1$ are presented in Figure 7. The tapes made from the slurries Ce-

Table 1. Comparison of the Properties of the Tapes Made from Different Slurries

composition	solid loading (wt %)	ceramic loading (wt %)	green tape density (g/cm ³)	tensile stress (Mpa)	firing shrinkage (xy)	firing shrinkage (z)
A ₂ B ₃ C ₂ D ₁	72.59	67.01	3.67	0.81	13.30%	19.30%
A ₃ B ₂ C ₂ D _{0.5}	72.86	65.32	3.65	0.58	16.70%	20.00%
A ₄ B ₁ C ₁ D ₁	71.29	64.00	3.35	1.84	17.30%	18.90%
A ₄ B ₁ C ₂ D ₁	71.22	63.41	3.37	1.05	17.50%	18.90%

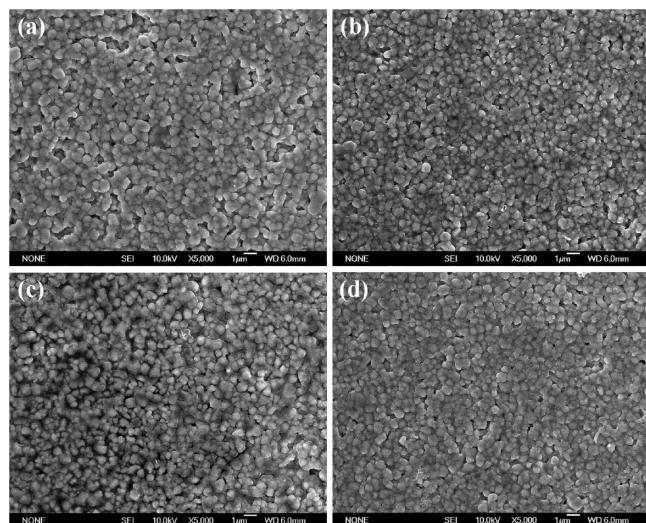


Figure 6. SEM images of the green tapes from the slurry (a) Cera₆₀Sol₂₀A₂B₃C₂D₁; (b) Cera₆₀Sol₂₀A₃B₂C₂D_{0.5}; (c) Cera₆₀Sol₂₀A₄B₁C₁D₁; and (d) Cera₆₀Sol₂₀A₄B₁C₂D₁.

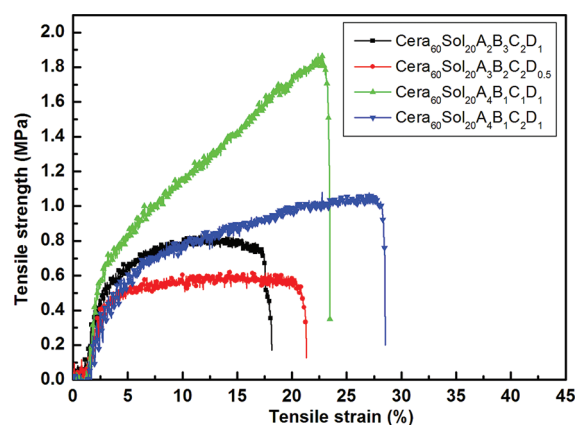


Figure 7. Tensile strength-strain curves of green tapes prepared with the Cera₆₀Sol₂₀A₂B₃C₂D₁, Cera₆₀Sol₂₀A₃B₂C₂D_{0.5}, Cera₆₀Sol₂₀A₄B₁C₁D₁, and Cera₆₀Sol₂₀A₄B₁C₂D₁ slurries.

ra₆₀Sol₂₀A₂B₃C₂D₁ and Cera₆₀Sol₂₀A₃B₂C₂D_{0.5} show lower tensile strength compared with that of the tapes made from the slurries Cera₆₀Sol₂₀A₄B₁C₁D₁, and Cera₆₀Sol₂₀A₄B₁C₂D₁. This should be due to the lower binder content and the high plasticizer/binder ratio. The tape made from the slurry Cera₆₀Sol₂₀A₄B₁C₁D₁ show the highest tensile strength of 1.84 MPa and a strain of about 24%, which indicates the good mechanical properties of the green tape made from the slurry Cera₆₀Sol₂₀A₄B₁C₁D₁. The tensile strength of the tape made from slurry Cera₆₀Sol₂₀A₄B₁C₂D₁ decreases to 1.05. But the strain increases to 28%. The strain increase contemporary with the strength decrease is the typical characteristic of increasing plasticizer in green tape.²⁵

To investigate the sintering performance of the green tapes, the tapes were dewaxed at 450 °C for 2 h and then calcined at 1050 °C for 4 h in air. All the sintered tapes are dense, and the morphology has no large difference. Figure 8 shows a typical

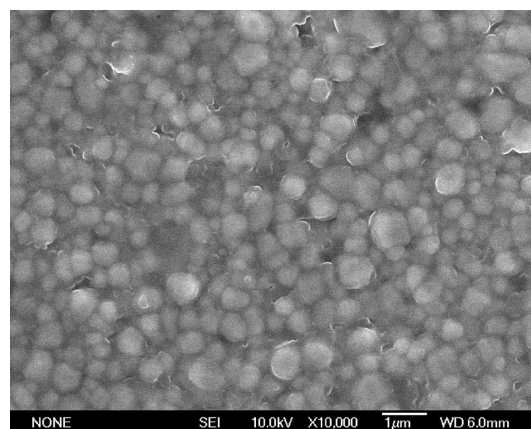


Figure 8. SEM image of the nature surface of the sintered ceramic tape made from Cera₆₀Sol₂₀A₄B₁C₁D₁ slurry.

SEM micrograph of the natural surface of the sintered tape made from Cera₆₀Sol₂₀A₄B₁C₁D₁ slurry. Cycle shaped grains with diameter less than 1 µm arrange compactly on the surface of the sintered tape. Considering the average particle size of 0.6 µm, there is no obvious grain growth after being sintered at 1050 °C for 4 h. The firing shrinkage of the tapes is listed in Table 1. The *xy*-axis shrinkage increases from 13.30% to 17.50% with the increase of the binder amount “*x*” from 2 to 4 g. However, the *z*-axis shrinkage has no obvious dependence on the binder amount. The tapes made from the slurries with binder amount of 4 g shows lower *z*-axis shrinkage of 18.90%, which is the lowest among the four kinds of tapes. The sintering behavior and other properties indicate that green tape made from Cera₆₀Sol₂₀A₄B₁C₁D₁ slurry is more suitable for the laminated components or device applications.

4. CONCLUSIONS

A kind of ethanol and ethyl-acetate binary solvent based ceramic tape-casting slurry was developed using the combinatorial approach. The combinatorial slurry library was designed considering the variation of the amount of binder, plasticizers, and dispersant, and prepared by a parallel magnetic stirring process. A two-step screening was carried out by investigating the segmentation and rheological characteristics of the slurries and the microstructure, mechanical property, sintering behavior of green tapes. A slurry system composed of ceramic powder/PVB/PEG 400/butyl-benzyl-phthalate/glyceryl triacetate was achieved suitable for making X7R dielectric ceramic green tapes. This combinatorial approach can be applied to develop a wide range of tape-casting slurries, colloids, and other composites.

■ ASSOCIATED CONTENT

● Supporting Information

Further details are given on source materials, library design, library preparation and characterization, and facilities and procedures for the second step screening. This material is available free of charge via the Internet at <http://pubs.acs.org>.

■ AUTHOR INFORMATION

Corresponding Author

*E-mail: liuzf@mail.sic.ac.cn (Z.L.), yxli@mail.sic.ac.cn (Y.L.).

Funding

The financial supports are from the Science and Technology Commission of Shanghai Municipality (No. 10dz1140300, STCSM-AM No. 09520714500), and the Guangdong Science and Technology Department (GDSTC, No. 2009A090100006, 2010B090300016).

■ REFERENCES

- (1) Twiname, E. R.; Mistler, R. E. *Tape casting: theory and practice*; The American Ceramic Society: Westerville, OH, 2000.
- (2) Thorel, A. Tape Casting Ceramics for High Temperature Fuel Cell Applications. In *Ceramic Materials*; Wunderlich, W., Ed.; Intech: Rijeka, Croatia, 2010; pp 49–67.
- (3) Gongora-Rubio, M. R.; Espinoza-Vallejos, P.; Sola-Laguna, L.; Santiago-Avilés, J. J. Overview of low temperature co-fired ceramics tape technology for meso-system technology (MsST). *Sen. Actuators, A* 2005, 89, 222–241.
- (4) Montgomery, D. C. *Design and Analysis of Experiments*, 6 ed; John Wiley & Sons: New York, 2004.
- (5) Rocak, D.; Kosec, M.; Degen, A. Ceramic suspension optimization using factorial design of experiments. *J. Eur. Ceram. Soc.* 2002, 22, 391–395.
- (6) Mei, S.; Yang, J.; Maria, J.; Ferreira, F.; Martins, R. Optimisation of parameters for aqueous tape-casting of cordierite-based glass ceramics by taguchi method. *Mater. Sci. Eng., A* 2002, 334, 11–18.
- (7) Besendorfer, G.; Roosen, A. Factors influencing the green body properties and shrinkage tolerance of LTCC green tapes. *Int. J. Appl. Ceram. Technol.* 2007, 4, 53–59.
- (8) Besendorfer, G.; Roosen, A. Particle shape and size effects on anisotropic shrinkage in tape-cast ceramic layers. *J. Am. Ceram. Soc.* 2008, 91, 2514–2520.
- (9) Yoon, D. H.; Lee, B. I. Processing of barium titanate tapes with different binders for MLCC applications- Part I: Optimization using design of experiments. *J. Eur. Ceram. Soc.* 2004, 24, 739–752.
- (10) Xiang, X. D.; Sun, X.; Briceño, G.; Lou, Y.; Wang, K.; Chang, H.; Wallace-Freedman, W. G.; Chen, S. W.; Schultz, P. G. A combinatorial approach to materials discovery. *Science* 1995, 268, 1738–1740.
- (11) Danielson, E.; Devenney, M.; Giaquinta, D. M.; Golden, J. H.; Haushalter, R. C.; McFarland, E. W.; Poojary, D. M.; Reaves, C. M.; Weinberg, W. H.; Wu, X. D. A rare-earth phosphor containing one-dimensional chains identified through combinatorial methods. *Science* 1998, 279, 837–839.
- (12) Chen, L.; Fu, Y.; Zhang, G.; Bao, J.; Gao, C. Optimization of Pr^{3+} , Tb^{3+} and Sm^{3+} co-doped $(\text{Y}_{0.65}\text{Gd}_{0.35})\text{BO}_3:\text{Eu}^{3+}_{0.05}$ VUV phosphors through combinatorial approach. *J. Comb. Chem.* 2008, 10, 401–404.
- (13) Su, X.; Zhang, K.; Liu, Q.; Zhong, H.; Shi, Y.; Pan, Y. Combinatorial optimization of $(\text{Lu}_{1-x}\text{Gd}_x)_3\text{Al}_5\text{O}_{12}:\text{Ce}_{3y}$ yellow phosphors as precursors for ceramic scintillators. *ACS Comb. Sci.* 2011, 13, 79–83.
- (14) Cong, P.; Dehestani, A.; Doolen, R.; Giaquinta, D. M.; Guan, S.; Markov, V.; Poojary, D.; Self, K.; Turner, H.; Weinberg, W. H. Combinatorial discovery of oxidative dehydrogenation catalysts within the Mo-V-Nb-O system. *Proc. Natl. Acad. Sci. U.S.A.* 1999, 96, 11077–11080.
- (15) Cui, J.; Chu, Y. S.; Famodu, O. O.; Furuya, Y.; Hatrick-Simpers, J.; James, R. D.; Ludwig, A.; Thienhaus, S.; Wuttig, M.; Zhang, Z.; Takeuchi, I. Combinatorial search of thermoelastic shape-memory alloys with extremely small hysteresis width. *Nat. Mater.* 2006, 5, 286–290.
- (16) Pullara, R. C.; Zhang, Y.; Chen, L.; Yang, S.; Evans, J. R. G.; Petrova, P. K.; Salak, A. N.; Kiselev, D. A.; Kholkin, A. L.; Ferreira, V. M.; Alford, N. McN. Manufacture and measurement of combinatorial libraries of dielectric ceramics: Part II. Dielectric measurements of $\text{Ba}_{1-x}\text{Sr}_x\text{TiO}_3$ libraries. *J. Eur. Ceram. Soc.* 2007, 27, 4437–4443.
- (17) Liu, G.; Wolfman, J.; Autret-Lambert, C.; Sakai, J.; Roger, S.; Gervais, M.; Gervais, F. Microstructural and dielectric properties of $\text{Ba}_{0.6}\text{Sr}_{0.4}\text{Ti}_{1-x}\text{Zr}_x\text{O}_3$ based combinatorial thin film capacitors library. *J. Appl. Phys.* 2010, 108, 114108–1–6.
- (18) Fujino, S.; Murakami, M.; Varatharajan, A.; Lim, S. H.; Nagarajan, V.; Fennie, C. J.; Wuttig, M.; Salamanca-Riba, L.; Takeuchi, I. Combinatorial discovery of a lead-free morphotropic phase boundary in a thin-film piezoelectric perovskite. *Appl. Phys. Lett.* 2008, 92, 202904–3.
- (19) Hu, W.; Tan, X.; Rajan, K. Combinatorial processing libraries for bulk $\text{BiFeO}_3\text{-PbTiO}_3$ piezoelectric ceramics. *Appl. Phys. A: Mater. Sci. Process.* 2010, 99, 427–431.
- (20) Tseng, W. J.; Lin, C. L. Effect of poly-vinyl-butylal on the rheological properties of BaTiO_3 powder in ethanol–isopropanol mixtures. *Mater. Lett.* 2002, 57, 223–228.
- (21) Cutler, E. A.; Kleinlein, B. Effect of the hydroxyl content and molecular weight of poly-vinyl-butylal on tape properties. *J. Eur. Ceram. Soc.* 2009, 29, 3211–3218.
- (22) Lewis, J. A. Colloidal processing of ceramics. *J. Am. Ceram. Soc.* 2000, 83, 2341–2359.
- (23) Gomes, C. M.; Rambo, C. R.; Oliveira, A. P. N.; Hotza, D.; Gouvea, D.; Travitzky, N.; Greil, P. Colloidal processing of glass-ceramics for laminated object manufacturing. *J. Am. Ceram. Soc.* 2009, 92, 1186–1191.
- (24) Kim, D. H.; Lim, K. Y.; Paik, U.; Jung, Y. G. Effects of chemical structure and molecular weight of plasticizer on physical properties of green tape in $\text{BaTiO}_3/\text{PVB}$ system. *J. Eur. Ceram. Soc.* 2004, 24, 733–738.
- (25) Descamps, M.; Ringuet, G.; Leger, D.; Thierry, B. Tape casting: relationship between organic constituents and the physical and mechanical properties of tapes. *J. Eur. Ceram. Soc.* 1995, 15, 357–362.